UC Berkeley
Indoor Environmental Quality (IEQ)

Title

A model of heat and moisture transfer through clothing integrated with the UC Berkeley comfort model

Permalink

Authors

Fu, Ming
Yu, Tiefeng
Zhang, Hui
et al.

Publication Date

2014-06-01

Peer reviewed

A model of heat and moisture transfer through clothing integrated with the UC Berkeley Comfort model

Ming Fu[a]*, Tiefeng Yu[b], Hui Zhang[b], Edward Arens[b], Wenguo Weng[a], Hongyong Yuan[a]

[a] Institute of Public Safety Research, Department of Engineering Physics, Tsinghua University, Beijing, 100084, China.
[b] Center for Built and Environment, University of California, Berkeley. CA 94720, USA.

Corresponding information: +86-10-62796323   fm10@mails.tsinghua.edu.cn

Abstract

A detailed model of heat and moisture transfer through clothing has been developed and implemented in the multi-segment UC Berkeley Thermophysiological Comfort model (BTCM). Equations are presented for two paths of heat and moisture transfer, between naked skin and environment, and clothed skin and environment. Transient behavior due to absorption and desorption by clothing is included. Segment-specific values for clothing insulation, vapor resistance, and the effects of air movement and walking are estimated from various sources. The new model is shown to simulate results from empirical studies with good accuracy. Parametric simulations are done to evaluate the physiological and comfort influences of the airspeed correction equations, and the heat transfer effects of different clothing levels at different temperatures. The results quantify the substantial air velocity and air temperature impacts on thermal physiology and thermal comfort. It can be seen that the new model is useful for studying heat and moisture transfer through clothing, and evaluating thermal comfort in transient environments.

Keywords

Comfort model, Thermal comfort, Thermal sensation, Clothing, Heat transfer, Moisture transfer.

Nomenclature

A area (m^2)

C specific heat (J/(kg^{o}C))

F_{nude} fraction of segment area naked (dimensionless)

$F_{clothed}$ fraction of segment area clothed (dimensionless)

f_{clo} clothing area factor (dimensionless)

h heat transfer coefficient (W/(m^{2o}C))

I thermal resistance (m^{2o}C/W, clo)

k correction factor (dimensionless)

Le Lewis constant (16.5 ^{o}C/kPa)

M metabolic heat production (W)

m mass rate (kg/(m^{2}s))

P water vapor pressure (kPa)

q heat storage or heat loss (W,W/m^2)

Re vapor resistance (kPa m^{2}W^{-1})

T temperature (^{o}C)

t time (s)

v relative air velocity (m/s)

w wettedness (dimensionless, a fraction from 0 to1)

Greek symbols

λ enthalpy of water vaporization (2256 kJ/kg)

Subscripts

air   air

c   convection

clo   clothing

corr   corrected

env   environment

evap   evaporation

fat   fat

H_2O H_2O (water)

nude   naked skin

sat   saturated

skin   skin

storage   storage

sw   sweating

tot   total

vf   view factor

1. Introduction

Thermal psychological models of the human body have great importance with the concept of local sensation and thermal comfort [1-2]. The thermal sensation and comfort are mainly based on the local skin and core temperatures [3-5]. Those models of human thermoregulation can predict the local skin and core temperatures, along with heat and moisture transfer between the human body and environment, hence evaluating the local and overall thermal sensation and comfort [2].

The UC Berkeley Thermophysiological Comfort model (BTCM) developed by Huizenga et al. [1] includes several improvements over the Stolwijk physiological model [6] from which it was derived. The BTCM model has 16 body segments whose areas correspond to a widely used electrical manikin [7]. Each of these segments is simulated as four body layers (core, muscle, fat, and skin tissues) and a clothing layer. A separate series of nodes represents the transport of heat by blood flow between segments, including the effect of countercurrent heat exchange between paired arteries and veins in the limbs. Each of the body segments is radiatively, convectively, and (where applicable) conductively coupled to a model of the surroundings.

The BTCM model's simulated segment skin and core temperatures are used to also predict perceived thermal sensation and comfort, for each segment and for the whole body (e.g. hand sensation cold or hot, whole-body cold or hot, etc.), using an embedded set of sensation and comfort models developed by Zhang [3-5]. The BTCM model has been validated against empirical physiological responses in transient, non-uniform thermal environments [1].

However, the treatment of clothing insulation in the BTCM model has been insufficient for the purposes of the model, which include predicting dynamic sensible and evaporative heat transfer for each body segment under a range of wind and walking conditions. This paper describes the new clothing model, compares its predictions to manikin studies of clothing insulation under wind, and to human

subject tests of human thermal physiology.

The original clothing model calculated moisture absorption/desorption in the clothing using the regain approach [8-9]. This assumed the moisture content of the clothing to be at equilibrium with the relative humidity in the air. However, equilibrium with the environment is often not reached in transient thermal environments [10]. The clothing absorption/desorption needs to be considered as part of the model.

In addition, the heat and moisture transfer through the air layer surrounding the clothing varied with airspeed using coefficients from manikin experiments in a wind tunnel [11], therefore, the thermal insulation and vapor resistance within the clothing layer are in fact affected by the relative air movement as well as by the air motion caused by walking [12].

The new clothing model considers, for each body segment, the effect of clothing moisture absorption/desorption rate on heat transfer, as well as the effect of airspeed on the thermal and vapor resistance of clothing. It is based on a whole-body unsteady-state thermal model for clothing from Jones and Ogawa [13], combined with airspeed corrections derived from ISO 9920 [14]. In simulating a particular garment or an ensemble of garments, the BTCM requires local clothing properties specific to each of the body segments. These segment-level properties must be simulated based on several sources, given that empirical data are not yet complete.

The clothing model is described below, compared with recent empirical clothing data, and used to compare comfort effects for different ambient velocity levels, air temperatures and clothing ensembles.

2. Mathematical formulation

The existing physiology, thermal regulation, blood flow, and radiant exchange models of the BTCM

model remain unchanged. The following describes only the modeling of heat and moisture from skin and through clothing to the air.

As shown in Fig. 1, two paths are considered through which heat is transferred from exposed skin or clothed skin to ambient air. The sum fraction of naked and clothed area of each segment is 1.

$$F_{nude} + F_{clothed} = 1 \tag{1}$$

Where F_{nude} and $F_{clothed}$ are the fractions of the segment area that are naked and clothed, respectively. When this segment is totally nude, the clothed fraction is zero.
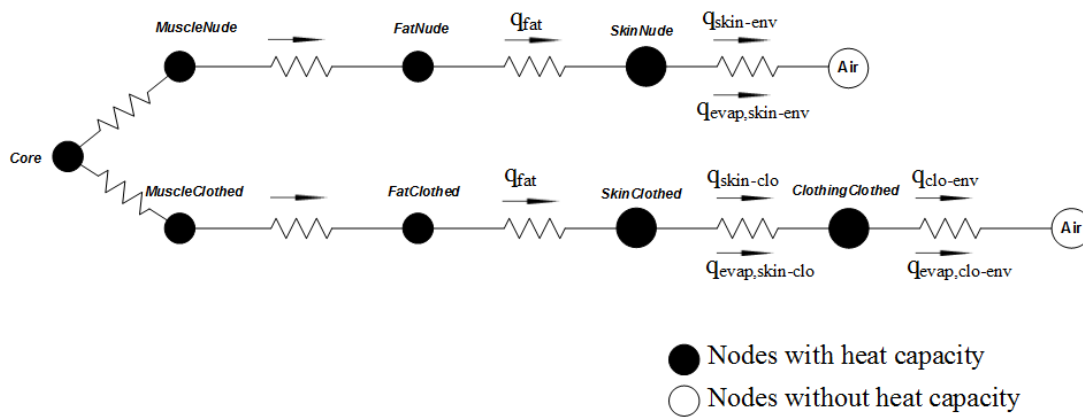
Fig.1. Node network.

2.1 Skin node

For the skin node, the stored heat within the skin is the heat gain from the inner body layers and metabolic heat production, subtracting the heat loss from conduction, convection and radiation with the clothing or the environment, and the heat loss from sweating evaporation and absorption within clothing. The heat transfer by conduction is described in [15], and is not considered in this paper. The stored heat within the skin, $q_{skin,storage}$, is:

$$q_{skin,storage} = q_{fat} + M_{skin} - q_{skin-env} - q_{skin-clo} - q_{evap,\,skin-env} - q_{evap,\,skin-clo} \tag{2}$$

Where q_{fat} and M_{skin} are the heat gain from fat and skin metabolic heat production, respectively, as

calculated by the BTCM model [1]. $q_{skin-env}$ is the sensible heat loss from nude skin to the environment, and $q_{skin-clo}$ is the sensible heat loss from clothed skin to the clothing. $q_{evap, skin-env}$ and $q_{evap, skin-clo}$ are the latent heat exchange between skin and environment from the naked skin, and between skin and clothing from the clothed skin, respectively. $q_{skin-env}$ and $q_{evap, skin-env}$ are zero when the segment is covered entirely by clothing, and $q_{skin-clo}$ and $q_{evap, skin-clo}$ are zero when the segment is entirely nude.

2.1.1 Sensible heat transfer

The BTCM model separates $q_{skin-env}$ into convection and radiative heat transfer. Convective heat transfer is influenced by the air velocity and air temperature near each segment. View factors between each body segment and surrounding surfaces are used to calculate the radiative heat transfer in non-uniform environments [1]. $q_{skin-env}$ is calculated as:

$$q_{skin-env} = A * F_{nude} * \left(h_c \left(T_{skin} - T_{air} \right) + q_{vf-skin} \right) \tag{3}$$

Where A is the total skin surface area of the segment. T_{skin} and T_{air} are the skin and ambient air temperatures, respectively (^{o}C). $q_{vf-skin}$ is the radiative heat transfer calculated by view factors, W/m^2, which is described in [1]. h_c is the coefficient of the convective heat exchange, (W·m^{-2}·^{o}C^{-1}), determined for each segment by de Dear et al. [16].

$q_{s k i n}$ is obtained by the temperature difference between skin and the clothing (T_{clo}). I_{clo} is the number of clo unit for the intrinsic thermal resistance of the clothing (1 clo = 0.155 m^{2}KW^{-1}):

$$q_{skin-clo} = A * F_{clothed} * \frac{\left(T_{skin} - T_{clo} \right)}{I_{clo}} \tag{4}$$

2.1.2 Moisture transport

In this paper, the moisture transport is modelled as a one-dimensional flow through clothing located

between the skin and the environment. Water absorption/desorption by clothing is lumped as changing the weight of the garment.

The latent heat exchange from the naked skin to environment, $q_{evap,\,skin-env}$ can be calculated by:

$$q_{evap,skin-env} = w * A * F_{nude} * \frac{\left(P_{skin} - P_{air}\right)}{R_{e,air}} \tag{5}$$

Where P_{skin} and P_{air} are the partial vapor pressures at skin and in the air, respectively, kPa. w is the skin wettedness, calculated by BTCM. $R_{e,air}$ is the evaporative resistance of ambient air (kPa·m²·W⁻¹). $R_{e,air}$ is related to h_c through the Lewis constant for air (Le, 16.5 °C/kPa).

$$R_{e,air} = \frac{1}{h_c * Le} \tag{6}$$

The vapor pressure at the sweat glands on the skin surface is the saturated value for the skin temperature [13]. Therefore, the vapor pressure at the skin surface, P_{skin} can be calculated as [13]:

$$P_{skin} = \frac{\dfrac{P_{skin,sat}}{R_{e,skin}} + \dfrac{\lambda_{H_2O}}{A * F_{nude}} m_{sw} + \dfrac{P_{air}}{R_{e,air}}}{\dfrac{1}{R_{e,air}} + \dfrac{1}{R_{e,skin}}} \qquad \text{for the naked skin} \tag{7a}$$

$$P_{skin} = \frac{\dfrac{P_{skin,sat}}{R_{e,skin}} + \dfrac{\lambda_{H_2O}}{A * F_{clothed}} m_{sw} + \dfrac{P_{air}}{R_{e,tot}}}{\dfrac{1}{R_{e,tot}} + \dfrac{1}{R_{e,skin}}} \qquad \text{for the clothed skin} \tag{7b}$$

Where λ_{H_2O} is the enthalpy of water vaporization, 2256 kJ/kg. m_{sw} is the rate of sweat production (kg/m²s), as obtained from the BTCM model [1]. $R_{e,skin}$ is the evaporative resistance of the skin, 0.33 kPa·m²·W⁻¹ for a well hydrated person [17]. $R_{e,tot}$ is the total evaporative resistance of clothing (kPa·m²·W⁻¹), including the intrinsic evaporative resistance of clothing, $R_{e,clo}$ and $R_{e,air}$.

$$R_{e,tot} = R_{e,clo} + \frac{R_{e,air}}{f_{clo}} \tag{8}$$

$f_{c\,l}$ is the clothing area factor, from McCullough et al. [18]. f_{clo} relates to I_{clo} as below:

$$f_{clo} = \begin{cases} 1 + 0.2I_{clo} & I_{clo} < 0.5\text{clo} \\ 1.05 + 0.1I_{clo} & I_{clo} \geq 0.5\text{clo} \end{cases} \tag{9}$$

P_{skin} is the saturated vapor pressure at the skin temperature and can be calculated by [17]:

$$P_{skin,sat} = \frac{1}{10}\exp\left(18.956 - \frac{4030.183}{T_{skin} + 235}\right) \tag{10}$$

The sweat amount on the skin surface does not exceed the limit of 35 gm^{-2} [13]. An excess amount of sweat is absorbed by the clothing in the clothed area or dripped from the nude area. For the clothed area, the moisture production from skin sweating equals the sum of moisture absorbed by the clothing, m_{clo} and moisture evaporation transferred through the clothing [13]:

$$m_{sw} = m_{clo,cloth} + \frac{\left(P_{skin,sat} - P_{air}\right)}{\lambda_{\text{H}_2\text{O}} * R_{e,tot}} \tag{11}$$

The latent heat exchange from the clothed skin to the clothing, $q_{evap,\,skin-clo}$ is calculated as below. $C_{\text{H}_2\text{O}}$ is the specific heat of water, 4.2×10^3J kg^{-1}ºC^{-1}.

$$q_{evap,skin-clo} = A * F_{clothed} * \left[\frac{\left(P_{skin} - P_{air}\right)}{R_{e,tot}} + C_{\text{H}_2\text{O}} * m_{clo,cloth}\left(T_{skin} - T_{clo}\right)\right] \tag{12}$$

2.2 Clothing node

The heat storage of the clothing node is calculated as:

$$q_{clo,storage} = q_{skin-clo} - q_{clo-env} + q_{evap,\,skin-clo} - q_{evap,clo-env} \tag{13}$$

Where $q_{clo-env}$ and $q_{evap,\,clo-env}$ are the sensible and latent heat loss between the clothing node and the environment, respectively.

$$q_{clo-env} = A * f_{clo} * F_{clothed}\left(h_c\left(T_{clo} - T_{air}\right) + q_{vf-skin}\right) \tag{14}$$

$$q_{evap,clo-env} = A * f_{clo} * F_{clothed} * \frac{\left(P_{cloth} - P_{air}\right)}{R_{e,air}} \tag{15}$$

The water from sweating is absorbed by the clothing when the skin is saturated, i.e. calculated P_{skin}

(Eq. 7) exceeds or equals the saturated vapor pressure $P_{skin,sat}$. Therefore, the temperature increase of the clothing with the absorbed water is obtained as below, where C_{clo} is the specific heat of clothing, J kg^{-1} ^{o}C^{-1}.

$$\Delta T_{clo} = \frac{q_{clo,storage}}{A\left(C_{clo}m_{clo} + C_{H_2O}*F_{clothed}*m_{clo,cloth}\right)}$$
(16)

2.3 Segment-specific clothing thermal insulation and vapor resistance

The thermal insulation and vapor resistance of clothing determine heat and moisture transfer for a clothed person. The ISO 9920 database [14] summarizes the thermal insulation and vapor resistance of clothing ensembles for work and daily wear. The database only provides whole-body resistances. For a multi-segment model such as the BTCM, data for local sensible and latent heat transfer resistances are needed.

We have measured sensible heat transfer resistance for local body segments (Lee et al. [19]) using the Madsen segmented thermal manikin that corresponds directly to the BTCM simulated manikin [6]. Other segment-level clo values have been published by Havenith et al. [20]. Wang et al. [21] studied localised evaporative resistance of clothing using sweating thermal manikins. The effects of air and body movements on localised evaporative resistance of clothing were examined. However, Wang et al. [21] only provided the boundary air layer's localised evaporative resistance and the correction factors for localised clothing evaporative resistance, not the localised clothing evaporative resistance. In addition, in the study of Wang et al. [21], only three sets of one-layer light clothing ensembles were tested. More experiments with clothing for winter are required. Wang et al. are currently measuring with 15 types of clothing, to provide a database for the localised permeability index for the clothing layer, and the localised thermal insulation and evaporative resistance of clothing (personal commutation). ISO

9920 gives a ratio of vapor resistance to thermal insulation of 0.18 for most one- or two-layer clothing ensembles [14]. We applied this ratio to local clo values to obtain a vapor resistance for each segment. In future study, we will apply the new database from the study of Wang et al.

Two typical indoor clothing ensembles (for summer and winter) are described here, from [19]. The summer clothing (0.6 *clo* overall) consists of cotton shirt with long sleeves, cotton thin trousers, and shoes. The winter indoor clothing (1.27 *clo* overall) consists of cotton shirt and cotton sweater, thick cotton long pants, socks and shoes. In both ensembles, the head and hands are nude. The local thermal insulations and vapor resistances of the two types of clothing are shown in Table 1.

Table 1. Thermal properties of the summer and winter clothing ensembles.

Segment	Summer		Winter indoor	
	Thermal resistance (*clo*)	Evaporative resistance (m²kPa/W)	Thermal resistance (*clo*)	Evaporative resistance (m²kPa/W)
Head	0	0	0	0
Chest	1.10	0.198	2.79	0.502
Back	0.90	0.162	2.27	0.409
Pelvis	0.93	0.167	1.76	0.317
Upper arm	0.74	0.133	1.90	0.342
Lower arm	0.41	0.073	1.39	0.250
Hand	0	0	0	0
Thigh	0.49	0.088	0.95	0.171
Lower leg	0.48	0.086	0.70	0.126
Foot	0.49	0.088	0.88	0.158

2.4 Effects of air movement on clothing thermal insulation and vapor resistance

Thermal insulation and vapor resistance are reduced by convection caused by external air movement and by body movement [10, 22]. Correction equations for air movement and walking are provided in ISO 9920 [14] for relative air velocity >0.15 m/s based on wind-tunnel/manikin studies by Havenith et al. [11]. In these equations (Eqs. 17-18), the correction to vapor resistance relies on the correction to

thermal insulation. The equations apply only to the whole body.

$$I_{clo,corr} = k_{clo,corr} * I_{clo} = \exp\left[-0.281(v_{air} - 0.15) + 0.044(v_{air} - 0.15)^2 - 0.492v_w + 0.176v_w^2\right] * I_{clo} \qquad (17)$$

$$R_{e,clo,corr} = \left[0.3 - 0.5k_{clo,corr} + 1.2k_{clo,corr}^2\right] * R_{e,clo} \qquad (18)$$

where $I_{clo,corr}$ and $R_{e,clo,corr}$ are the airspeed-corrected thermal insulation and vapor resistance of the clothing, respectively. $k_{clo,corr}$ is the correction factor for the thermal insulation of clothing, v_{air} is the relative air velocity, m/s, and v_w is the walking speed, m/s.

Oguro et al. [23] determined air movement effects on segment-specific clothing insulation, from 0 to 5 m/s. He did not examine vapor resistance or effects of walking. He used the same wind tunnel and thermal manikin [6] that de Dear et al. [17] had employed earlier to develop the segment nude skin heat transfer coefficients used in the BTCM model. Only one ensemble was tested, trousers and long-sleeved shirt, with overall *clo* equal to 0.6. Regression models for clothing insulation were developed for all segment parts.

Table 2 shows air movement correction factors for the segment parts and the whole body, as measured or calculated by Oguro et al. [23], Havenith et al. [20], and ISO 9920 [14]. Under relative air velocity less than 1 m/s, the difference of the correction factor between each segment found by Oguro et al. [23], Havenith et al. [20], and the whole-body by ISO 9920 [14] is very small. At 1 m/s, ISO 9920 [14] and [23] predict similar insulation reductions. Somehow the overall reduction for [20] is significantly larger than for the other two (closer to Oguro's values for 2 m/s). At relative air velocity above 1 m/s, ISO 9920 predicts slightly bigger reduction than Oguro [23]. This might be because Oguro taped the clothing at the boundaries of the body segments, to eliminate inter-segment heat transfer from taking place laterally underneath the clothing. This restriction could increase the overall insulation under air movement.

Table 2 also addresses walking. It includes a comparison between the ISO 9920 correction for whole-body and the [20] corrections for individual body segments. The corrections for the extremities are greater than for the trunk and inner limbs.

Table 2. Corrections to thermal insulation for local segment parts [20, 23] and the whole body [14].

Segment	Clothing correction factor for						
	relative air velocity (m/s)						walking speed (1m/s)
	0.4 [23]	0.4 [20]	1 [23]	1 [20]	1.5 [23]	2 [23]	1 [20]
Head	--		--		--	--	--
Chest	0.92	0.86	0.81	0.65	0.76	0.72	0.82
Back	0.94	0.96	0.86	0.81	0.82	0.79	0.86
Pelvis	0.94	0.89	0.85	0.72	0.81	0.79	0.80
Upper arm	0.91	0.89	0.78	0.71	0.73	0.69	0.75
Lower arm	0.91	0.89	0.79	0.70	0.74	0.70	0.63
Hand	--		--	--	--	--	--
Thigh	0.92	0.95	0.81	0.80	0.76	0.72	0.71
Lower leg	0.93	0.96	0.85	0.86	0.81	0.78	0.69
Foot	0.96	0.95	0.91	0.85	0.89	0.87	0.69
Whole body [20,23]	0.92	0.90	0.81	0.69	0.77	0.73	0.74
Whole body [14]	0.94		0.81		0.74	0.69	0.73

Note: in [20], the ASTM and G3 ensembles are used for relative air velocity and walking corrections, respectively. The [20] buttock and abdomen values are averaged to provide the 'pelvis' value in the table.

Because the individual and overall correction factors calculated by Oguro et al. [23] are close to the ISO overall value [14], we conclude that it is reasonable to use the ISO 9920 equations (Eqs.17-18) to determine the correction for relative air velocity on the thermal resistance of each individual body segment. But the amount of correction might be underestimated for higher relative air velocity by the ISO equations when compared to Havenith's new data [20], which includes a limited number of Western

ensembles that can be compared with ISO 9920. These differences are currently unexplained.

For walking, BTCM also uses the ISO equation for all individual body segments, which unavoidably overestimates the correction for the trunk section and underestimates the correction for the extremities. The errors are acceptable until more measured data becomes available. For non-Western ensembles one can now obtain segment-specific correction factors for air movement and walking [20].

We cannot do the same validation for segment-specific vapor resistance, but because the ISO 9920 vapor correction depends generally on the air movement effect on thermal resistance, it seems reasonable to assume that applying the ISO 9920 overall vapor correction to each segment's thermal resistance should be valid.

3. Results and discussion

3.1 Validation of the developed model

The physical variables in the BTCM model may be compared to field study results in which the clothed subjects were exposed to temperature step changes. Parametric runs are made of thermal and sensation behavior after a step change to show the dynamic sensitivity of the sensible and vapor heat transfer model, and of the air movement correction.

BTCM model predictions were compared with measured sensible and latent heat loss data from Jones and Ogawa [13]. The subjects with the activity level of 1 met were first exposed to a cold environment of 4.4 °C and 50 % RH for 45 min, and then stayed in an environmental chamber at 21.1 °C and 50 % RH for 60 min. Fig. 2 shows the measured sensible and latent heat loss from the clothed body to the environment, compared to published simulated results from the human-clothing model of George Fu [24] (G.Fu), and from the BTCM with the new clothing model. The BTCM model simulation agrees well with the experimental data.
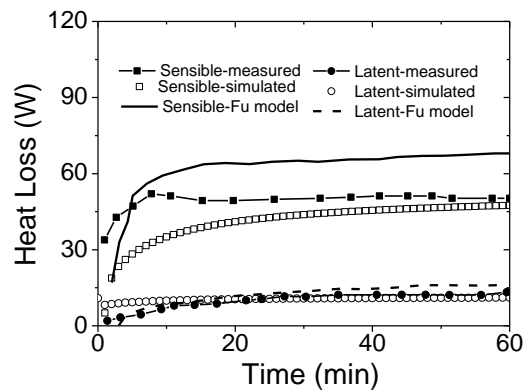
Fig.2. Comparison of measured sensible and latent heat losses (Jones and Ogawa [13]), with simulated results from the G. Fu [24] and BTCM models. Experimental conditions: 21.1 °C and 50% RH, following a step change after 4.4 °C and 50 % RH.

BTCM model results were also compared with measured data of Kakitsuba [25]. The subjects (dressed in 100% cotton T-shirt and short pants) rested in an environment at 28 °C and 50 RH for 30 min, followed by a hot exposure at 40 °C and 50 RH for 60 min. The core (rectal) temperature, mean skin temperature, and the clothing temperature for the trunk were reported during the hot exposure period at 40 °C [25]. Fig. 3 shows the comparison of the experimental measurements and the predicted values of the BTCM model. The predicted core, mean skin and clothing temperature are consistent with the measured data, with a maximum difference of 0.9 °C occurring in skin temperature.
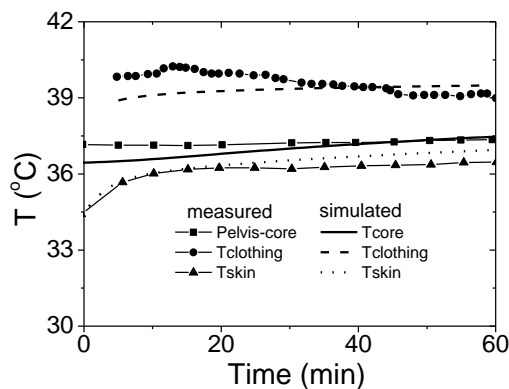
Fig. 3. Comparison of measured [25] with simulated core, skin and clothing temperatures during a step

change to a hot exposure period at 40 ^{o}C.

3.2 Analysis of the effects of air movement on heat transfer in clothing

To assess the effects of relative air velocity, thermal physiology and thermal comfort were simulated with and without the segment-level clothing-airspeed correction factors. A quietly standing person dressed in summer long-sleeve clothing (0.6 *clo*) is exposed for 120 min to 30 ^{o}C, 50 RH and a range of relative air velocities (0.1-2.0 m/s).

Fig. 4(a-e) shows the distribution of averaged skin and core temperatures, overall thermal sensation and comfort, and averaged heat loss from skin to the environment. It can be seen that the skin and core temperatures decrease with relative air velocity, and the heat loss to the environment increases.

There is no airspeed correction for thermal insulation and vapor resistance between 0 and 0.15 m/s, the limit for still air within the model. At above 0.5 m/s, the corrected skin and core temperatures are less than those without correction (Fig.4 (a-b)). The correction effect is small at 0.5 m/s, but increases with relative air velocity. At 2 m/s, the skin and core temperature difference between with- and without airspeed correction is 0.67 and 0.25 ^{o}C, respectively, and the heat loss to the environment is increasing with airspeed correction (Equations (3-4 and 14-15)). The corrections to clothing insulation and vapor resistance have a large effect on the body's thermal physiology.

In Fig.4 (c-d), the whole-body thermal sensation decreases from hot to neutral with increasing the relative air velocity, while comfort increases with the relative air velocity (overall comfort going from -2 or less, to -0.5 or more). Taking the relative air velocity of 1.5m/s as an example, the correction factor velocity $k_{clo,corr}$ is 0.7. The corresponding overall sensations are 1.3 without correction and 0.45 with

correction, a significant difference on the sensation scale. Overall comfort is also changed significantly

by adding the airspeed correction, from -0.47 to 0.56.

(a) skin temperature

(b) core temperature

(c) sensation

(d) comfort

(e) heat flux
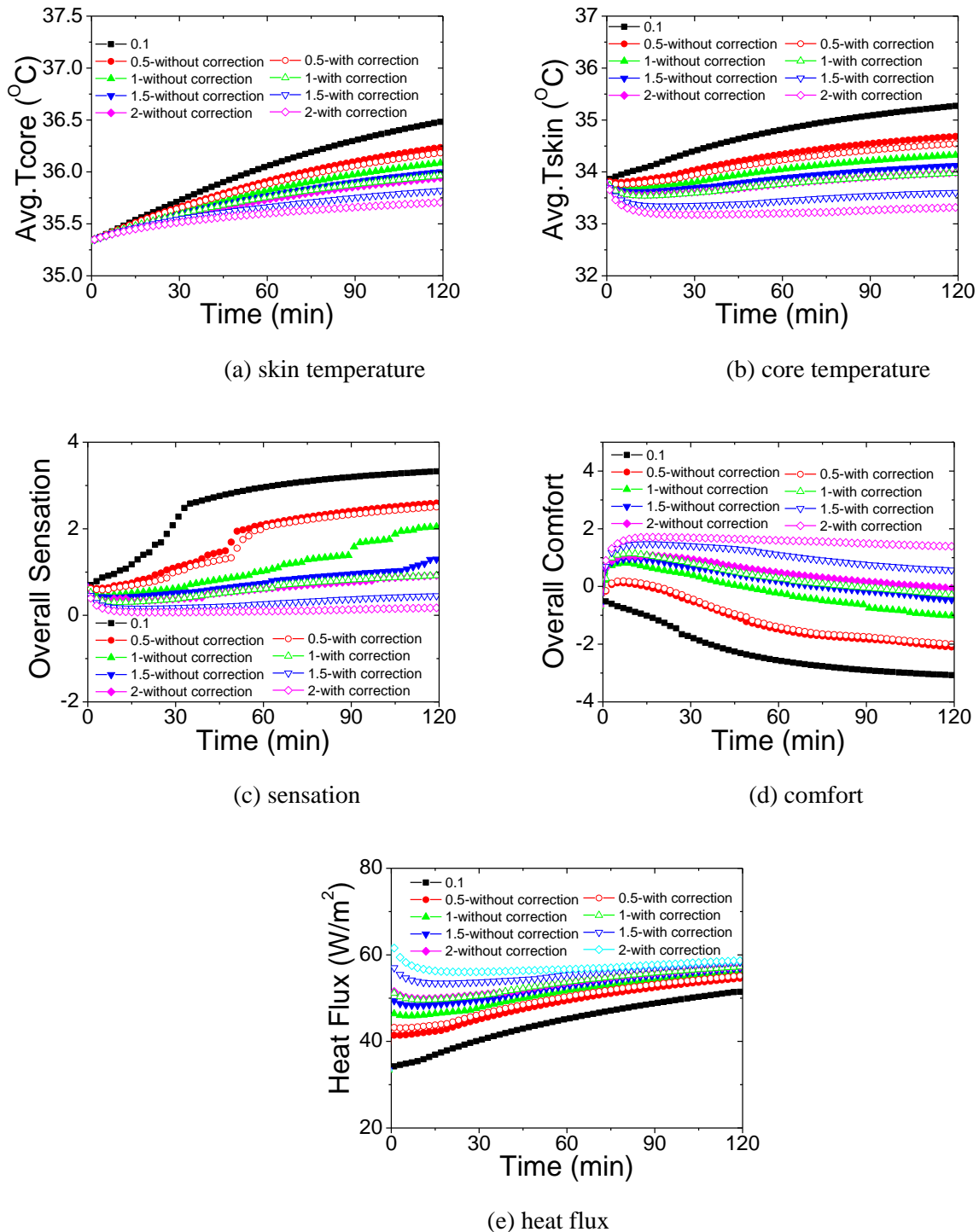
Fig. 4. Comparison of averaged skin and core temperature, overall thermal sensation and comfort, and

averaged heat loss, at 30 ^{o}C with and without correction for relative air velocity (unit: m/s).

3.3 Analysis of the effects of air temperature and clothing level

The model is next used to examine the effects of air temperature and clothing on physiology, comfort, and heat flux. An assumed person (dressed in summer clothing and in winter indoor clothing, respectively) is quietly standing (met rate of 1.1) in still air (0.1 m/s) for 120 min. According to ASHRAE Standard 55 [26], 50% RH is usually used in modeling about a subject wearing clothing standardized for the activity concerned with the same air temperature and thermoregulatory strain (skin wettedness).Therefore, the effect of RH on heat and moisture through clothing is not considered as an important issue in this study.

Indoor air temperatures in the range of 15 - 30 $^{\circ}$C are common in naturally ventilated buildings [26]. Fig. 5 shows the temperature distribution of averaged skin and core temperatures, overall thermal sensation and comfort, and averaged heat loss, under different air temperatures. It can be seen that the skin and core temperatures increase as the air temperature increases from 15 to 30 $^{\circ}$C, along with a decrease in heat loss to the environment (seen in Fig.5 (a,b,e)).

From Fig.5 (c-d), with the increase of air temperature from 15 to 30 $^{\circ}$C, the overall temperature sensation rises from feeling cold (-3 or less) to feeling hot (+3 or more). Over time, the relatively abrupt drop occurring at 50–60 minutes for winter clothing at 25 $^{\circ}$C is a consequence of the piecewise sensation model switching modes as it enters the neutral range (a similar effect in the other direction is seen in Fig. 4(c)). In addition, a deficiency of predicting overall sensation by Zhang et al. [3-5] was caused by the discontinuity in the sensation model [27]. A sudden jump in overall sensation might appear even if the environment condition was smoothly changing [27], which was caused by transitions in the piecewise formulation of the comfort models described in [3-5]. Therefore, the occurrence of this effect is independent of the clothing model. The overall comfort first increases from cold discomfort to slight

comfort (at the neutral temperature near 25 °C), then decreases into hot discomfort as the temperature continues to rise. These values are close to responses observed in lab and field studies.

(a) core temperature

(b) skin temperature

(c) sensation

(d) comfort

(e) heat flux
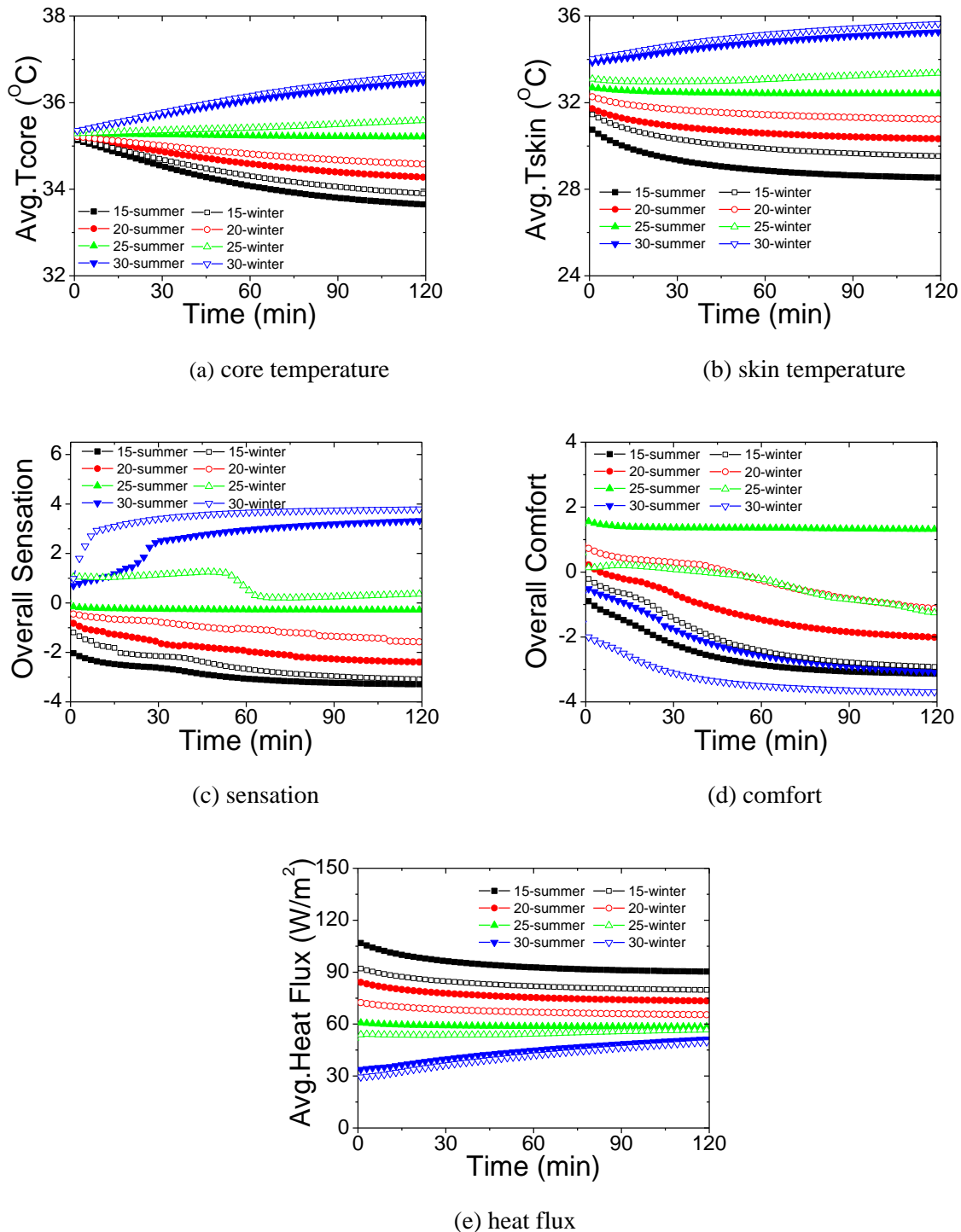
Fig. 5. Comparison of averaged skin and core temperature, overall thermal sensation and comfort, and averaged heat loss, in summer and winter clothing under different air temperatures (unit: °C).

Comparing different clothing types (summer and winter indoor clothing), the skin and core temperatures for winter indoor clothing can be seen to be more than those for summer clothing. At 25 ${}^{\circ}$C, the body feels neutral in summer clothing but feels slightly warm in winter clothing. The figures show that the combined influence of clothing insulation and vapor resistance significantly affects both thermal physiology and thermal sensation/comfort in transient thermal environments.

(a) Latent heat loss   (b) Sensible heat loss
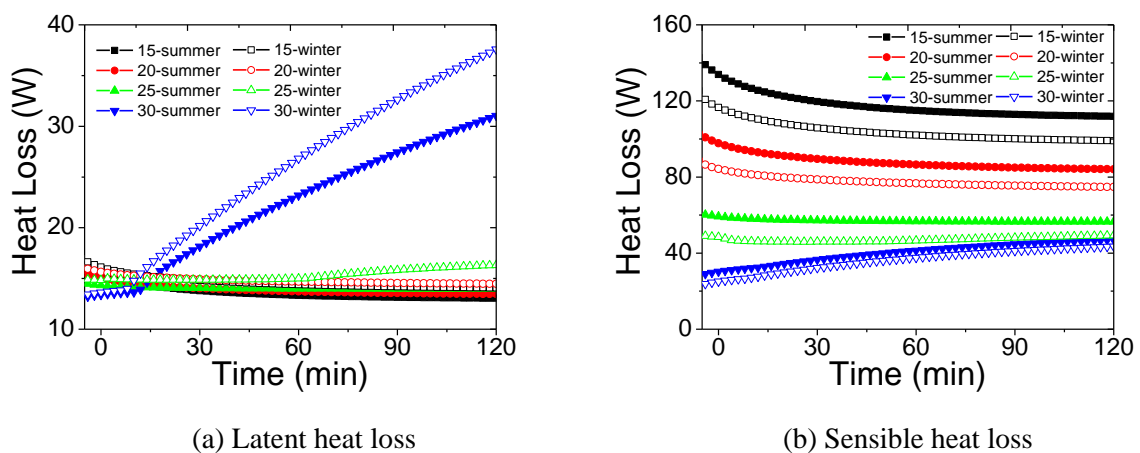
Fig. 6. Latent and sensible heat loss from skin in summer and winter clothing under different air temperatures (unit: ${}^{\circ}$C).

The sensible and latent heat loss from skin under different air temperatures are shown separately in Figure 6. It can be seen in Fig.6(a) that the latent heat loss does not increase very much as the air temperature increases from 15 to 25 ${}^{\circ}$C. However as the air temperature reaches 30 ${}^{\circ}$C, the latent heat loss at 120 minutes is 2.4 times as much as the value for 25 ${}^{\circ}$C. This reflects the onset of sweating between 25 and 30 ${}^{\circ}$C. The thicker winter clothing does not impede the latent heat loss, but increases it by elevating the body's sweat rate.

From Fig. 6(b), the sensible heat loss decreases as the air temperature increases from 15 to 30 ${}^{\circ}$C. One

can see that though winter clothing insulation as expected decreases the heat loss in cool environments relative to summer clothing, the effect almost ceases at 30 $^{\circ}$C as sweating lowers the skin temperature and latent heat transfer takes over.

4. Conclusions

In this paper, we have described a multi-segment clothing model that is integrated into the BTCM model. It is based on the whole-body model of Jones and Ogawa [13], modified to independently account for 16 body segments. Thermal insulation, vapor resistance, and moisture absorption/evaporation in clothing are considered for each body part. Two paths of heat and moisture transfer are described, between either naked or clothed skin and the environment, and the total heat flux for a segment is a function of the fractions of its area that are nude and clothed. Segment-specific effects of external air movement on the thermal insulation and vapor resistance of clothing are extrapolated using the whole-body insulation-correction equations in ISO 9920 [14], developed by Havenith et al. [20]. The ISO 9920 equations are tested against further clothing measurements by Oguro et al. [23] and Havenith et al. [20], and found to give a reasonable prediction of each segment's clothing under air motion, at least for a typical 0.6clo Western-style clothing ensemble. We conclude that the equations are suitable for Western clothing, at least until more segment-specific data can be obtained. Detailed segment-specific clothing and airspeed-correction data has recently been measured for non-Western ensembles, and these can be used directly in simulation.

The developed model is validated by comparing with results from tests of clothed human subjects. The simulation results of core, skin and clothing temperatures, and the sensible and latent heat loss from skin compare well with the experimental measurements.

The human thermal response and thermal comfort are then predicted and compared at different air velocity levels, and at different air temperatures with two typical clothing ensembles. The results quantify the substantial air velocity and air temperature impacts on thermal physiology and thermal comfort. The skin and core temperatures decrease with air speed and increase with the air temperature. The whole-body thermal sensation decreases from hot to neutral with increasing the relative air velocity, while comfort increases (whole-body going from uncomfortable to comfortable).

The developed model can be used to predict thermal physiology and thermal comfort with different clothing types under different thermal environments. This model can be used to evaluate thermal comfort in transient thermal environments, including office buildings, automobiles, and outdoors with different air velocities for each segment.

Acknowledgement

References

[1]   Huizenga C, Zhang H, Arens E. A model of human physiology and comfort for assessing complex thermal environments. Build Environ 2001; 36 (6):691-699.

[2]   Foda E, Almesri I, Awbi H, Sirén K. Models of human thermoregulation and the prediction of local and overall thermal sensations. Build Environ 2011; 46(10): 2023-2032.

[3]   Zhang H, Arens E, Huizenga C, Han T. Thermal sensation and comfort models for non-uniform and transient environments: Part I: Local sensation of individual body parts. Build Environ 2010;45(2): 380-388.

[4]   Zhang H, Arens E, Huizenga C, Han T. Thermal sensation and comfort models for non-uniform and transient environments, part II: Local comfort of individual body parts. Build Environ 2010;45(2): 389-398.

[5]   Zhang H, Arens E, Huizenga C, Han T. Thermal sensation and comfort models for non-uniform and transient environments, part III: Whole-body sensation and comfort. Build Environ 2010;45(2): 399-410.

[6]   Stolwijk JAJ. A Mathematical Model of Physiological Temperature Regulation in Man. NASA Report, 1970.

[7]   Madsen TL. Thermal Comfort Measurements. ASHRAE Trans 1976; 82(1):60-75.

[8]   Morton WE, Hearle JWS. Physical properties of textile fibres. Manchester. UK: The Textile Institute, 1993.

[9]   Voelker C, Hoffmann S, Kornadt O, Arens E, Zhang H, Huizenga C. Heat and moisture transfer through clothing. IBPSA Building Simulation, 2009, Glasgow, Scotland.

[10] Havenith G, Richards MG, Wang XX, et al. Apparent latent heat of evaporation from clothing: attenuation and "heat pipe" effects. J Appl Physiol 2008;104(1):142-149.

[11] Havenith G, Holmér I, Den Hartog EA, Parsons KC. Clothing evaporative heat resistance-proposal for improved representation in standards and models. Ann Occup Hyg 1999; 43(5):339-346.

[12] Havenith G, Holmer I, Parsons K. Personal factors in thermal comfort assessment: clothing properties and metabolic heat production. Energy Build 2002; 34(6):581-591.

[13] Jones BW, Ogawa Y. Transient interaction between the human and the thermal environment. ASHRAE Trans 1992;98(1):189-195.

[14] ISO 9920. Ergonomics of the thermal environment - Estimation of thermal insulation and water vapour resistance of a clothing ensemble. International Organization for Standardization, Geneva, Switzerland, 2009.

[15] Fu M, Yu TF, Zhang H, Weng WG, Yuan HY. Heat and moisture transfer through clothing for a person with

contact surface. Indoor Air 2014, July 7-12, 2014, Hong Kong, China.

[16] de Dear RJ, Arens E, Zhang H, Oguro M. Convective and radiative heat transfer coefficients for individual human body segments. Int J Biometeorol 1997;40 (3):145–56.

[17] Salloum M, Ghaddar N, Ghali K. A new transient bioheat model of the human body and its integration to clothing models. Int J Therm Sci 2007;46(4): 371-384.

[18] McCullough EA, Jones BW, Huck J. A comprehensive data base for estimating clothing insulation. ASHRAE Trans 1985; 91: 29-47.

[19] Lee J, Zhang H, Arens E. Typical clothing ensemble insulation levels for sixteen body parts. Proceedings of the CLIMA Conference, June 2013. Retrieved from: http://escholarship.org/uc/item/18f0r375.

[20] Havenith G, Hodder S, Ouzzahra Y, Loveday D, Kuklane K, Lundgren K, et al. Report on manikin measurements for ASHRAE 1504-TRP. Extension of the Clothing Insulation Database for Standard 55 and ISO 7730 to provide data for Non-Western Clothing Ensembles, including data on the effect of posture and air movement on that insulation. ASHRAE, Atlanta, USA, 2013.

[21] Wang F, del Ferraro S, Lin L, Mayor T, Molinaro V, Ribeiro M, et al. Localised boundary air layer and clothing evaporative resistances for individual body segments. Ergonomics 2012; 55(7):799-812.

[22] Havenith G, Heus R, Lotens, WA. Clothing ventilation, vapour resistance and permeability index: changes due to posture, movement and wind. Ergonomics 1990; 33(8): 989-1005.

[23] Oguro M, Arens E, de Dear RJ, Zhang H, Katayama T. Convective heat transfer coefficients and clothing insulations for parts of the clothed human body under airflow conditions. Journal of Architectural Planning and Environmental Engineering, 2002; 561:21-29.

[24] Fu G. A transient, 3-D mathematical thermal model for clothed human. PhD dissertation, Kansas State University, USA, 1995.

[25] Kakitsuba N. Dynamic changes in sweat rates and evaporation rates through clothing during hot exposure. J Therm Biol 2004; 29 (7-8): 739–742.

[26] ASHRAE Standard 55-2013. Thermal environmental conditions for human occupancy. ASHRAE, Atlanta, USA, 2013.

[27] Zhao Y, Zhang H, Arens E, Zhao QC. Thermal sensation and comfort models for non-uniform and transient environments, part IV: Adaptive neutral setpoints and smoothed whole-body sensation model. Build Environ 2014;72: 300-308.